Supporting Information

Marked Increase in the Binding Strength between the Substrate and the Covalently Attached Monolayers of Zeolite Microcrystals by Lateral Molecular Cross-Linking between the Neighboring Microcrystals

By **Jin Seon Park, Yun-Jo Lee, and Kyung Byung Yoon***

Synthesis of Cubic Zeolite-A. The zeolite-A used in this study was synthesized from a gel whose composition was AIP:TEOS:TMAOH:NaCl:H_2O = 0.7:3:1.85:0.74:300, where, AIP, TEOS, and TMAOH represent aluminum isopropoxide, tetraethyl orthosilicate, and tetramethylammonium hydroxide, respectively. Distilled water (70 mL) was introduced into a plastic beaker containing TMAOH (Aldrich, 33.6 g, 25 wt%). AIP (Acros, 7.5 g) and TEOS (Acros, 33 g) were sequentially added to the aqueous solution of TMAOH and then stirred for 2 h for hydrolysis. An aqueous solution of sodium chloride (1.15 g NaCl dissolved in 90 mL of H_2O) was subsequently added into the solution and then stirred for 12 h. The top of the plastic beaker was covered with a piece of plastic film, and sealed with a rubber band. The plastic beaker was placed in an oven whose temperature was maintained at 100 °C. After elapse of 7 d, the beaker was removed from the oven, and fresh sodium chloride solution (1.15 g NaCl dissolved in 90 mL of H_2O) was added into the plastic beaker while the turbid solution was vigorously stirred. After wrapping the top, the plastic beaker was placed in the oven at 100 °C for 3 d. The resulting nearly monodisperse zeolite A crystals were purified by repeated washing and sedimentation cycle. The templates were removed from zeolite crystals prior to assembly for 12 h at 550 ^{o}C.

Preparation of AP-Tethering Zeolite-A (AP-Z). Zeolite-A microcrystals (100 mg) were introduced into a round-bottomed flask charged with toluene (15 mL) and the heterogeneous mixture was sonicated for 10 min to thoroughly disperse zeolite crystals in the solvent. (3-aminopropyl)triethoxysilane (APS, Aldrich, 0.3 mL) was introduced into the toluene suspension of zeolite crystals, and the heterogeneous mixture was refluxed for 1 h under argon. After cooling to room temperature the zeolite crystals were isolated by centrifugation, and washed with fresh anhydrous toluene. The centrifugation-wash cycle was repeated for additional 4 times, and the cycle was repeated for 5 times by employing ethanol as the solvent. The resulting zeolite crystals were dried under vacuum.

Preparation of AP-Tethering Glass Plates (AP-G) and TPDA-Tethering AP-G Plates (TPDA-AP-G) or 1,4-Diisocyanatobutane (DICB)-Tethering AP-G Plates (DICB-AP-G). A Teflon support mounting ten clean glass plates ($1.8 \times 1.8 \times 0.2$ mm^3) was placed in a round-bottomed flask charged with a toluene solution (50 mL) of APS (0.3 mL), and the solution was refluxed for 1 h under argon. After cooling to room temperature, the glass plates were removed from the flask, and washed with copious amounts of toluene. A Teflon support mounting ten AP-G plates was immersed into a concentrated toluene solution of TPDA (50 mL, 100 mM) contained in a round-bottomed flask, and the solution was refluxed for 3 h. The TPDA-AP-G plates were removed from the flask and then washed with toluene, chloroform, and finally with ethanol. The washed glass substrate was dried using a gentle stream of high purity nitrogen. DICB-AP-G was prepared according to the same method described above except substituting DICB with TPDA.

Monolayer Assembly of AP-Z on TPDA-AP-G or DICB-AP-G. Freshly prepared AP-Z (20 mg) and five TPDA-AP-G plates were introduced into a round-bottomed Schlenk flask containing 30 mL of toluene, and the mixture was refluxed for 2 h under argon. The zeolite-coated glass plates were removed from the flask, sonicated in fresh toluene for ~20 sec to remove any physisorbed zeolite crystals from the monolayers, washed with copious amounts of toluene, and dried by blowing a gentle stream of pure nitrogen. Monolayer Assembly of AP-Z on DICB-AP-G was carried out according to the same method described above except substituting DICB with TPDA.

Cross-Linking of the Closely-Packed, Neighboring AP-Z Microcrystals in the Monolayers with TPDA or DICB. Five glass plates coated with the monolayers of AP-Z microcrystals were introduced into a round-bottomed flask charged with a concentrated toluene solution of TPDA (50 mL, 100 mM), and the solution was refluxed for 3 h. The TPDA-treated monolayers were washed with copious amounts of toluene, chloroform, and ethanol. The washed cross-linked monolayers were dried by exposing to a gentle stream of high purity nitrogen.

Verification of the Presence of AP Groups on AP-Z and AP-G by Ninhydrin (NH) Test. Ninhydrin (NH) has often been used as the reagent for the identification of primary amines because it readily produces Ruhemann's Purple (RP) upon reaction with primary amines, which gives an intense purple color (eq 1), enabling the ready spectroscopic identification of its existence. The UV-vis spectra of NH and RP are shown in Figure SI-1A.

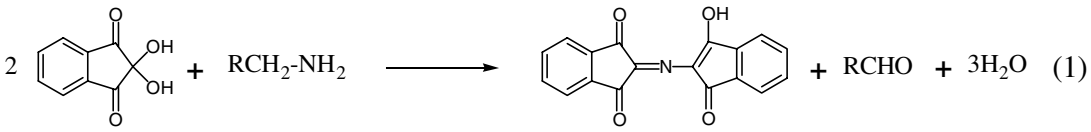

ninhydrin (NH)
(pale yellow)

Ruhemann's Purple (RP)
(purple)

We therefore employed NH for the detection of AP groups on zeolite surfaces and glass plates. For detection of AP groups on zeolite surfaces, the APS-treated zeolite-A (AP-Z) microcrystals (0.1 g) and NH (0.1 mg) were introduced into a round-bottomed flask charged with ethanol (20 mL), and the heterogeneous mixture was refluxed for 1 h. After reflux, the slurry turned pale purple. The UV-vis spectrum of the supernatant solution showed the characteristic absorption bands of RP at 405 and 570 nm as shown in Figure SI-1B, confirming that the APS-treated zeolite-A crystals indeed have AP groups on the surface. For the detection of AP-groups on the surfaces of APS-treated glass plates, three pieces of APS-treated glass (AP-G) plates were coated with an ethanol solution of NH (5 mM) by dipping and removing the plates into and from the solution. The NH-coated plates were then gently warmed using a heat gun. Because of the weak intensities of the absorption bands of RP on the glass plates resulting from the presence of very small amounts of AP groups on each glass plate, three glass plates were overlaid for spectrophotometric detection. Although weak, the three glass plates indeed showed the characteristic absorption bands of RP as shown in Figure SI-1C.

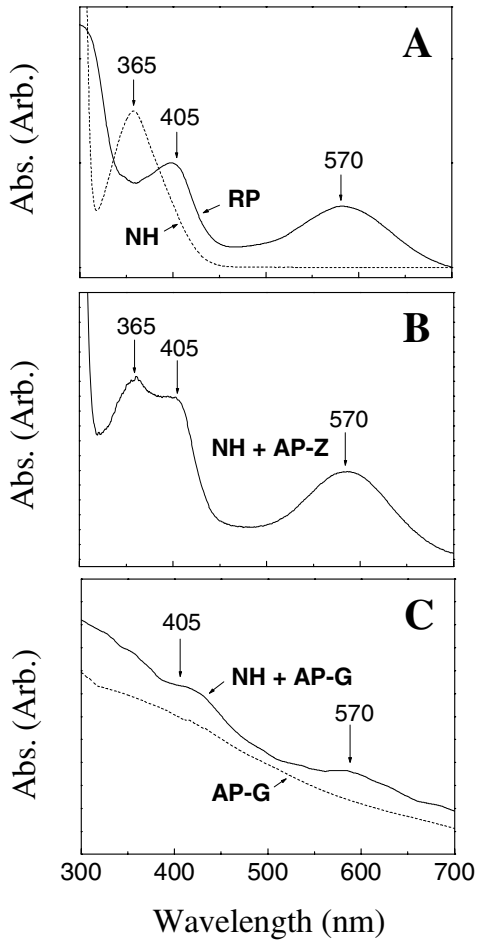

Figure SI-1. UV-vis absorption spectra of ethanol solutions of ninhydrin (NH) and Ruhemann's Purple (RP) (as indicated) (A), the supernatant solution from the refluxed mixture of NH and APS-treated zeolite-A in ethanol (B), and overlaid three pieces of NH-coated, APS-treated glass plates after exposure to warm wind (C).

Verification of the Presence of TPDA Groups on the AP-Tethering Fused Silica (AP-FS) Plates after Treatment with TPDA. TPDA has two strong absorption maximums at 258 and 265 nm, and a weak absorption at 300 nm in solution as shown in Figure SI-2A. As a means to detect the presence of TPDA groups on the AP-G plates after treatment of AP-G with TPDA we used fused silica (FS) plates instead of glass plates since FS is transparent in the UV region in which TPDA absorbs. Therefore, we coated FS plates with AP in the same way we did for the preparation of AP-G. The UV-vis spectrum of an AP-tethering FS (AP-FS) plate is shown in Figure SI-2B. As expected, AP groups did not absorb up to 200 nm. However, the TPDA-treated AP-FS (TPDA-AP-FS) showed a strong absorption band at ~265 nm and a weak shoulder band at ~330 nm, indicating the ready attachment of TPDA to the AP group via an imine linkage (Figure SI-2C). We ascribe the reason for the red shifts of the strong 258 and 265 nm bands to a broader, single 270 nm band and the weaker 300 nm band to 330 nm band to the reason that the one aldehyde and one imine groups, instead of two aldehyde groups, are attached to the phenyl ring upon attaching TPDA onto the surface-bound amino groups through imine linkages.

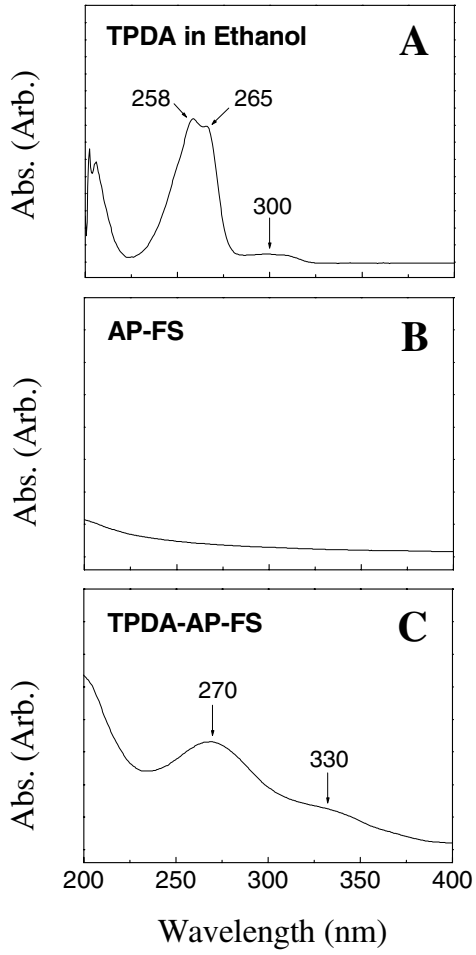

Figure SI-2. UV-vis absorption spectra of TPDA in ethanol (A), AP-FS (B), and TPDA-AP-FS (C).

Verification of the Presence of AP-groups on the Monolyares of AP-Z Microcrystals Assembled on TPDA-AP-G Plates. We also applied the NH test to detect the presence of AP groups on the AP-Z microcrsytals after assembly into monolayers on TPDA-AP-G plates. Thus, as typically shown in Figure SI-3, the diffuse reflectance spectra of the AP-Z monolayers on TPDA-AP-G plates did not show any absorption bands in the visible region. However, upon treating the monolayers with NH the characteristic bands of RP appeared at 405 and 570 nm, verifying that the surfaces of the AP-Z zeolite microcrystals were still coated with large numbers of AP groups after monolayer assembly.

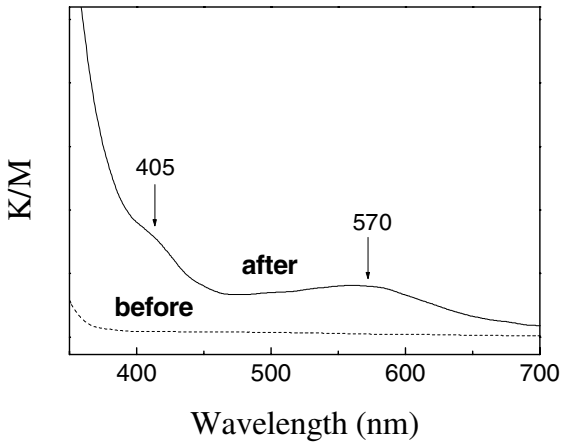

Figure SI-3. Diffuse reflectance UV-vis spectra of a monolayer of AP-Z microcrystals assembled on a TPDA-AP-G plate before and after treatment with NH (as indicated). K/M denotes Kubelka-Munk value.

Verification of the Presence of TPDA Groups on the Monolayers of AP-Z Microcrystals Assembled on TPDA-AP-G and TPDA-AP-FS after Cross-Linking the AP-Z Microcrystals with TPDA. To detect the presence of TPDA groups on the surfaces of AP-Z microcrystals after cross-linking them with TPDA, monolayers of AP-Z crystals were assembled on FS plates instead of glass according to the same procedure for the preparation of AP-Z monolayers on glass, and treated the monolayers with TPDA to cross-link the microcrystals. For the UV-vis analysis, the monolayers were coated with a small amount of DMSO (as an index matching fluid) to minimize the scattering of light from the AP-Z microcrystal faces. The UV-vis absorption spectra of AP-Z monolayers on TPDA-AP-FS showed a weak shoulder band with the onset at 325 nm as typically shown in Figure SI-4A (The strong absorption at the wavelength shorter than 250 nm is due to the absorption of DMSO). However, the TPDA-treated monolayers showed a strong absorption band at ~265 nm and a weak shoulder band at ~330 nm as typically shown in Figure SI-4A, indicating that the attachment of TPDA had readily occurred on the AP group via imine linkages as was observed in the case of TPDA-treated AP-FS (See

Figure SI-2C). Furthermore, the cross-linked monolayers of AP-Z on TPDA-AP-G plates were negative in the NH test as shown in Figure SI-4B, indicating the ready consumption of primary amine (AP) groups from the surface upon treatment with TPDA.

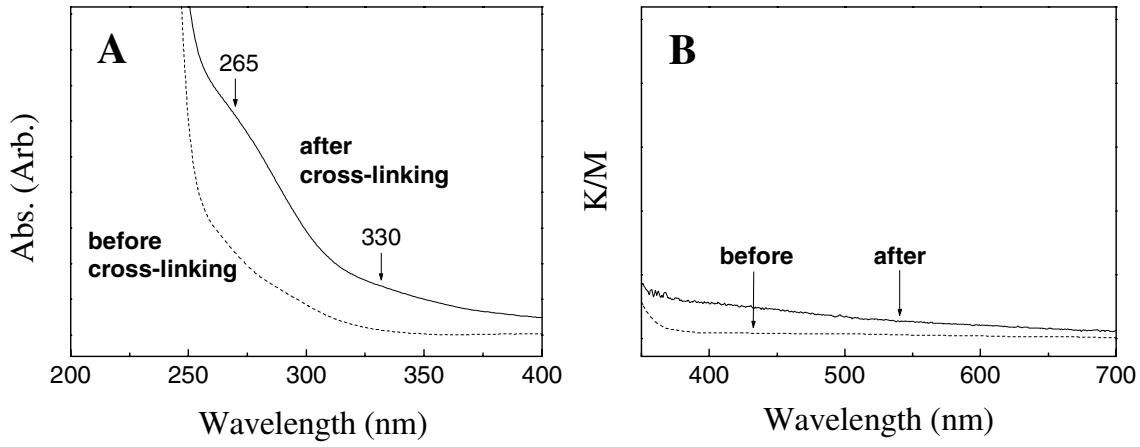

Figure SI-4. The UV-vis absorption spectra of the monolayers of AP-Z microcrystals assembled on TPDA-AP-FS plates before and after cross-linking (as indicated) between the surface-bound AP groups on the neighboring, closely packed zeolite microcrystals with TPDA (A) and the cross-linked monolayers of AP-Z microcrystals assembled on TPDA-AP-G plates before and after reaction with NH (as indicated) (B).

Verification of Cross-Linking the AP-Z Microcrystals with DICB by Grazing-Angle (80°) FT-IR Spectra. We have obtained grazing-angle FT-IR spectra of the zeolite monolayers assembled on DICB-AP-G before and after cross-linking the AP-Z crystals with DICB as the lateral molecular cross-linker between the AP-Z crystals in the monolayers and the difference spectrum (Figure SI-5A). For comparison, we obtained the FT-IR spectra of DICB (in the form of thin film on KBr plate, panel B) and the diurethane compound prepared by reacting DICB with *n*-propylamine (KBr pellet, panel C). As for a reference, we also prepared AP-tethering glass beads (AP-GB, size = 107 μm), and subsequently tethered DICB on AP-GB by treating them (200 mg) with a large excess of DICB (0.42 g, 100 mM) in toluene (30 mL). Because the contacting area between the large glass beads is negligible (as a result of dispersion of the glass beads in a large volume of toluene) and DICB is very reactive toward amino groups, it is most likely that almost all of the glass bead surfaces are covered with -$(CH_2)_3$-NH-CO-NH-$(CH_2)_4$-NCO. Accordingly, it is most likely that there are equal numbers of urea (NH-CO-NH) and NCO functional groups on the DICB-treated AP-GB (DICB-AP-GB) whereas there are more urea than NCO groups on the surfaces of cross-linked AP-Z monolayers. We also obtained the FT-IR spectra of both AP-GB and DICB-AP-GB and the corresponding difference spectrum. Indeed the difference FT-IR

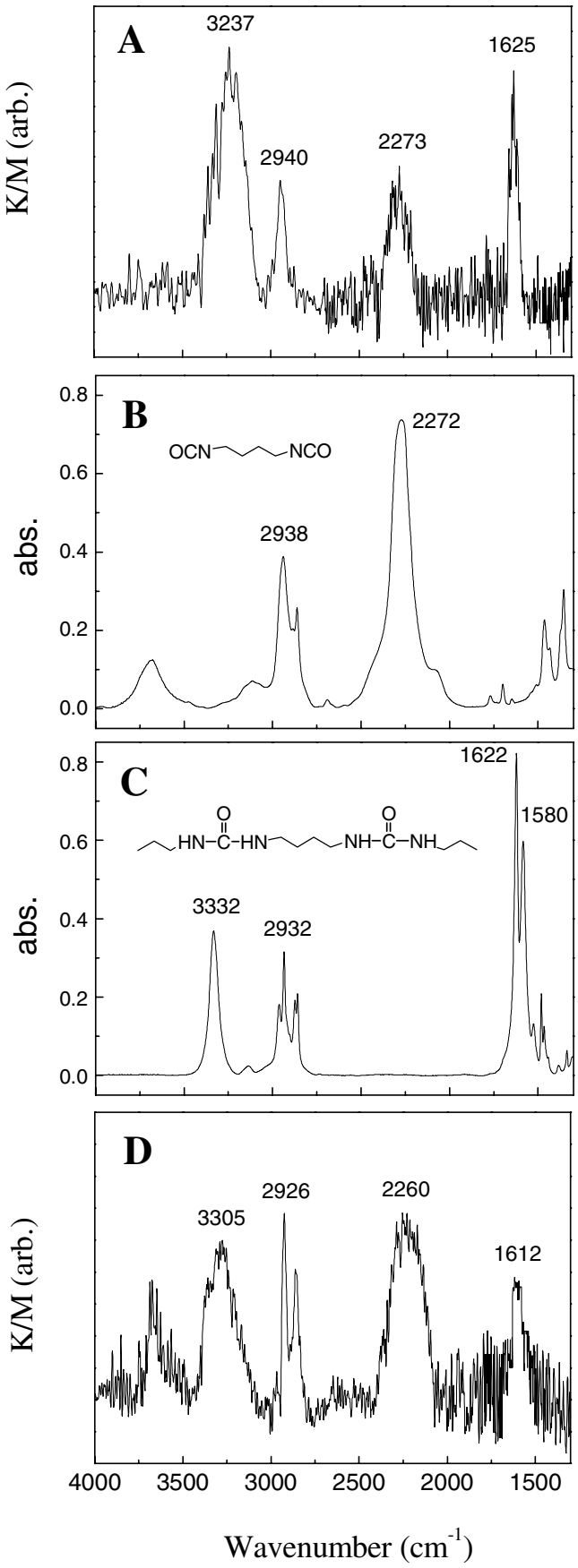

spectrum of cross-linked and uncross-linked AP-Z monolayers showed peaks at 3237, 2940, 2273, and 1625 cm^{-1} that are assignable to N-H, C-H, NCO, and C=O stretching bands by comparing with the authentic spectra shown in panels B and C. Most notably, the intensities of the N-H and C=O stretching bands in panel A are significantly higher than that of non-reacted (half-reacted) NCO stretching band, whereas those of N-H and C=O stretching bands in panel D are similar with that of NCO, indicating that there are more urea functional groups on the surfaces of cross-linked AP-Z monolayers. This suggests that later cross-linking indeed occurs between the closely packed AP-Z crystals upon treatment with DICB (and similarly with TPDA).

Figure SI-5. The difference FT-IR spectrum of the cross-linked and uncross-linked AP-Z monolayers (A), the FT-IR spectra of DICB (B) and diurea (C), and the difference FT-IR spectrum of DICB-AP-GB and AP-GB.

Effect of Zeolite Size on the Degree of Cross-Linking-Induced Increase in the Binding Strength. We repeated a new set of experiment using 300 nm-sized cubic zeolite-A crystals as the building blocks and TPDA as the vertical and lateral cross-linker. As was predicted, the effect the lateral cross-linking on the binding strength became much more prominent upon decreasing the size of zeolites from 1.7 μm to 300 nm. Figure SI-6 shows the SEM images of the AP-Z monolayers assembled on TPDA-AP-G before (panel A) and after lateral cross-linking (panel B), and after sonication for 5 (uncross-linked), 30 (cross-linked), 10 (uncross-linked), and 60 min (cross-linked). The detached amounts from the uncross-linked AP-Z monolayers were 18% and 47% after sonication for 5 and 10 min, respectively, whereas the detached amounts were 1.6% and 10% even after sonication of the cross-linked monolayers for much longer period of time, namely 30 and 60 min. The profiles of the average detached amounts with respect to time are shown in Figure SI-7. Thus, while the detached amount of uncross-linked monolayers reached 60% after sonication for 30 min that of cross-linked was only 1.6%. This corresponds to 38-fold increase in the binding strength upon cross-linking the 300-nm zeolite crystals, which is much larger than 7-fold increase observed in the case of 1.7-μm zeolite crystals. Such a remarkable cross-linking-induced increase in the binding strength upon decreasing the size of zeolite crystals is attributed to the decrease in the mass-to-surface area ratio. By the same analogy, it is interesting to note that the binding strength of the uncross-linked zeolite crystals is larger for 300-nm (smaller) than for 1.7 μm (larger) zeolite crystals. By extrapolation, we predict that the effect of lateral cross-linking on the binding strength will further increase with further decreasing the size of the building blocks to nanoparticles and to molecules.

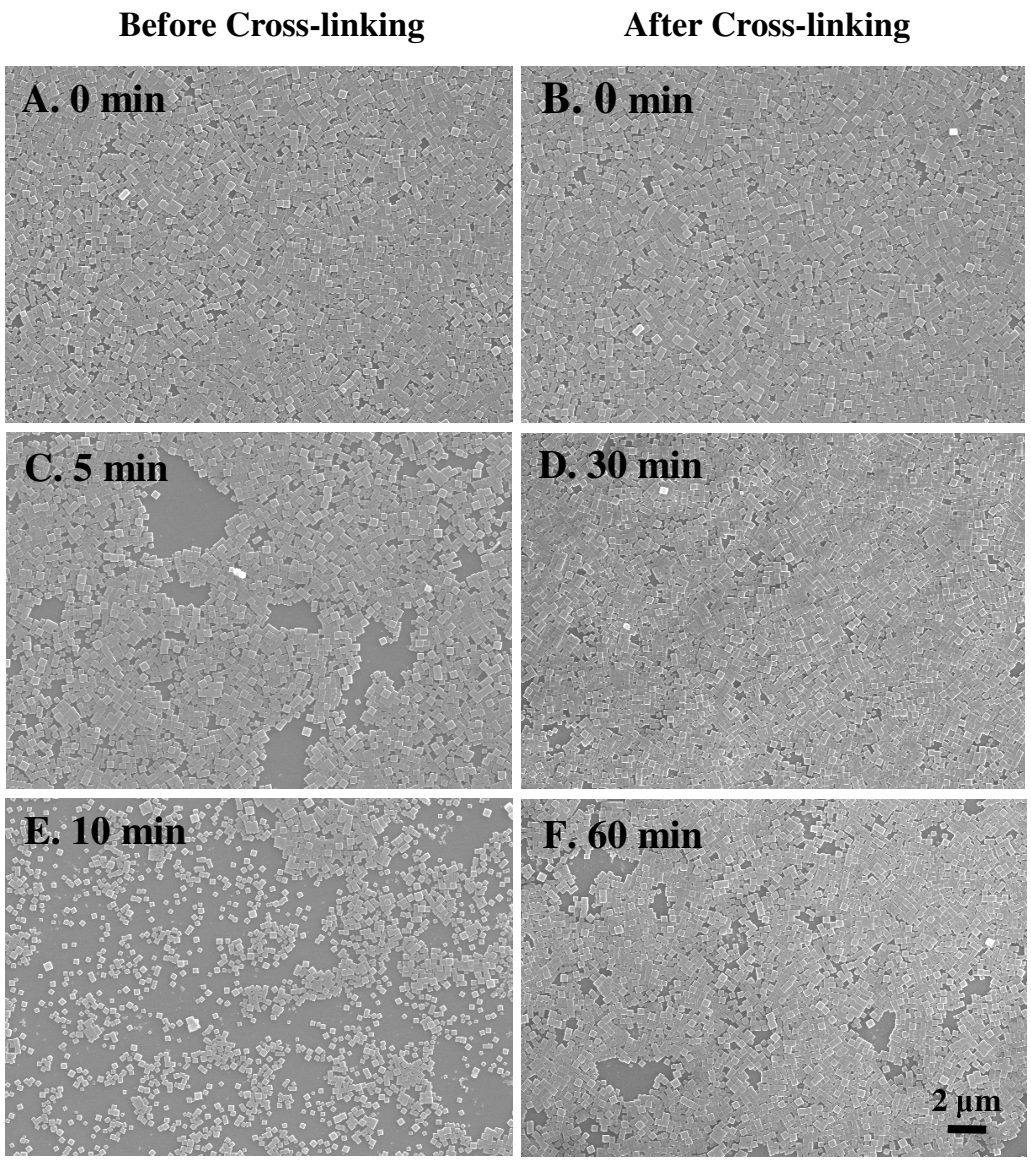

Figure SI-6. SEM images showing the uncross-linked (left) and cross-linked (right) monolayers of submicrometer-sized AP-Z crystals ($0.3 \times 0.3 \times 0.3$ μm^3)assembled on glass plates according to the schemes shown in Figure 1(text), and after sonication in toluene for the period indicated in each panel.

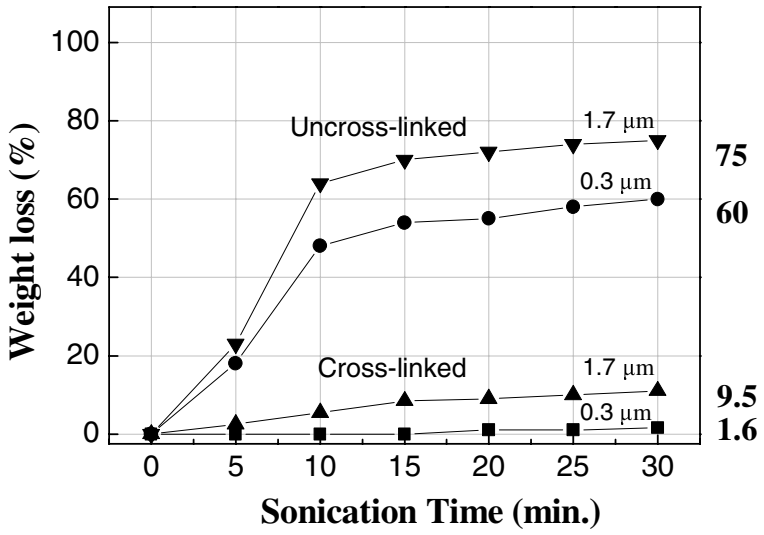

Figure SI-7. Average weight loss profiles of AP-Z crystals of two different sizes (as indicated) from the five monolayers assembled on glass plates with imine linkages before and after imine cross-linking (as indicated) with respect to sonication time.

Sonication-Induced Detachment Test. A zeolite-binding substrate was placed in a vial (i.d. = 2.4 cm) filled with 10 mL of toluene. The vial was then placed in an ultrasonic cleaning bath (22 x 12 x 11 cm) filled with 2.5 L of water, where the location of the vial was 6 cm above one of the two ultrasound generators (28 kHz, 95 W each) mounted under the bath. A stainless steel test tube rack was built into the bath to place the vial always in the same position. Each of the four legs of the rack was wrapped with a piece of 0.5-cm thick polyurethane sponge and the bottom and wall of the vial were enclosed with cotton cloth to minimize the transfer of severe vibration originating from the bottom of sonic bath to the vial through the rack. The water inside the bath was circulated through an external heat exchanger to keep the temperature constant (~25 °C). After each period of sonication, the substrate was removed from the vial and dried in an oven (120 °C) for 3 min, and the weight was measured on a microbalance (MT5, METTLER TOLEDO). For each run, fresh toluene was charged into the vial. After sonication for 30 min, the remaining zeolite crystals were completely removed from the substrate by rubbing it on a soft cloth, and the weight of the zeolite-free substrate was measured. The total weight of pure zeolite crystals bound to the substrate was deduced from the initial weight of the zeolite-binding substrate that was measured after sonication for 20 s to remove physisorbed crystals. Five independent runs were made and the resulting data were averaged. Since each substrate binds about 150 μg of zeolite crystals, a microbalance is sensitive enough to monitor the loss of zeolite crystals.